Half-wave plate systematics: impact on cosmic birefringence and component separation

---

Marta Monelli

Max Planck Institut für Astrophysik
Garching (Germany)

December 12th, 2022

searching for *B*-modes from inflation

Expectation: inflation-sourced perturbations leave traces on the CMB polarization.

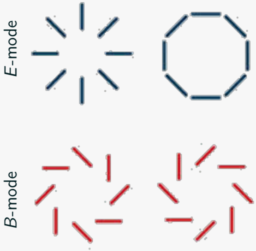

B-modes can probe inflation.

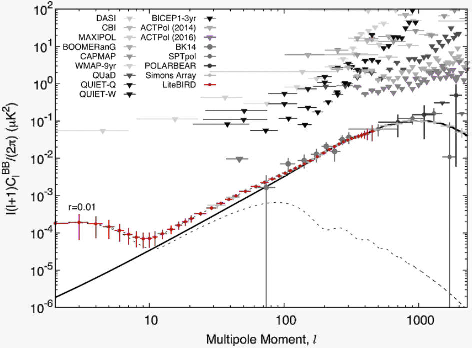

Unprecedented sensitivity requirements!

image credit: Hazumi et al (2019)

the HWP: reducing systematics

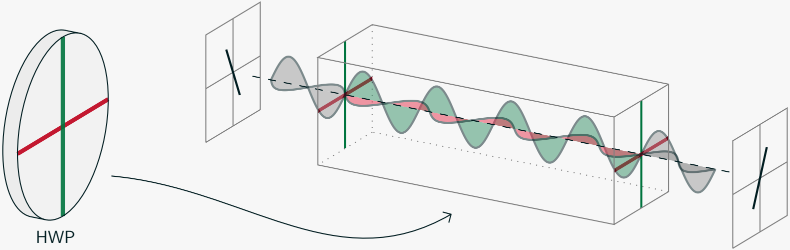

A **rotating** half-wave plate (HWP) as first optical element:

- modulates the signal to $4f_{\mathrm{HWP}}$, allowing to “escape” $1/f$ noise;
- makes possible for a single detector to measure polarization, reducing pair-differencing systematics.

the HWP: inducing systematics

Mueller calculus: radiation described as $S = (I, Q, U, V)$ and HWP effects parametrized by $\mathcal{M}_{\text{HWP}}$, so that $\mathrm{S}' = \mathcal{M}_{\text{HWP}}\mathrm{S}$.

$$\mathcal{M}_{\text{ideal}} = \begin{pmatrix} 1 & 0 & 0 & 0 \\ 0 & 1 & 0 & 0 \\ 0 & 0 & -1 & 0 \\ 0 & 0 & 0 & -1 \end{pmatrix}, \quad \mathcal{M}_{\text{HWP}} =$$

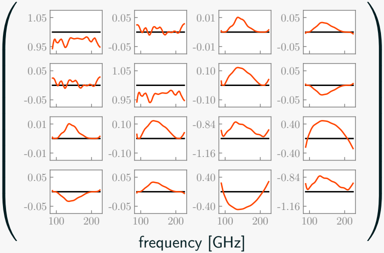

.

how does this affect the observed maps?

Giardiello et al. (2022) A&A 658

steps we took in that direction

- produce output maps from `beamconv`-based TOD simulations;
- derive analytic formulae to interpret the output;
- discuss how the non-idealities affect cosmic birefringence.

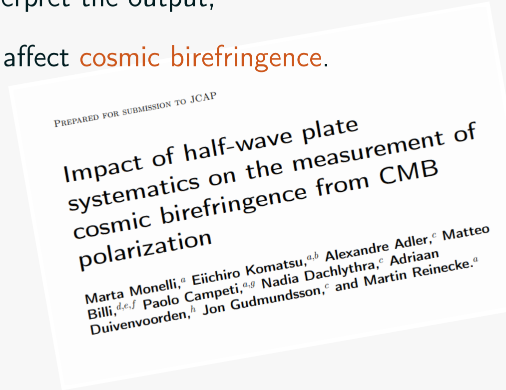

PREPARED FOR SUBMISSION TO JCAP

Impact of half-wave plate systematics on the measurement of cosmic birefringence from CMB polarization

Marta Monelli,[a] Eiichiro Komatsu,[a,b] Alexandre Adler,[c] Matteo Billi,[d,e,f] Paolo Campeti,[a,g] Nadia Dachlythra,[c] Adriaan Duivenvoorden,[h] Jon Gudmundsson,[c] and Martin Reinecke.[a]

Duivenvoorden et al. (2021) MNRAS 502; Monelli et al. `arXiv:2211.05685`

simulations

simulation input

Working assumptions: no noise, single freq., CMB-only, simple beams.

- I, Q and U **input maps** ($n_{\text{side}} = 512$) from best-fit 2018 Planck power spectra;
- 1 year of LiteBIRD-like **scanning strategy** (mimicking `pyScan`).
- **Instrument specifics**: 160 detectors from the 140 GHz channel of LiteBIRD's MFT.
- Non-ideal **HWP**: Mueller matrix elements from Giardiello et al. (2022) A&A 658.

specs.	values
f_{samp}	19 Hz
HWP rpm	39
FWHM	30.8 arcmin
offset quats.	[...]

ideal vs non-ideal output spectra

ideal and non-ideal TODs, both processed with **ideal** map-maker.

ideal vs non-ideal output spectra

ideal and non-ideal TODs, both processed with **ideal** map-maker.

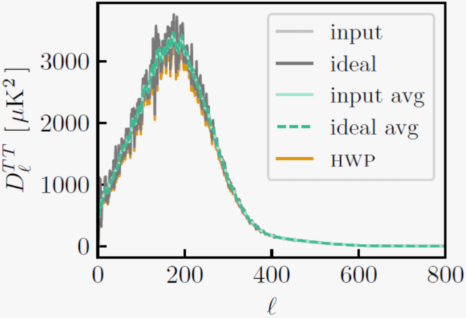

(beam transfer function not deconvolved)

- *TT* slightly affected

ideal vs non-ideal output spectra

ideal and non-ideal TODs, both processed with **ideal** map-maker.

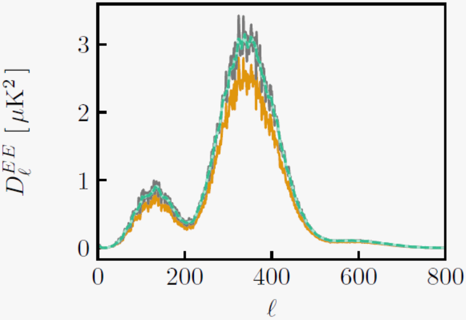

(beam transfer function not deconvolved)

- *TT* slightly affected
- *EE* lost power

ideal vs non-ideal output spectra

ideal and non-ideal TODs, both processed with **ideal** map-maker.

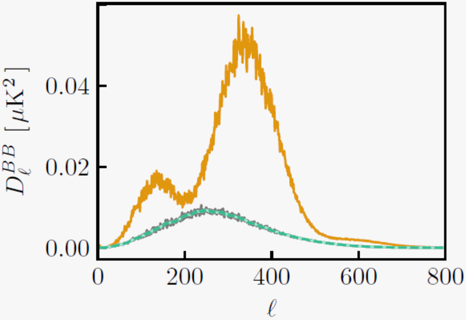

(beam transfer function not deconvolved)

- *TT* slightly affected
- *EE* lost power
- *BB* much larger (*EE* shape)

ideal vs non-ideal output spectra

ideal and non-ideal TODs, both processed with **ideal** map-maker.

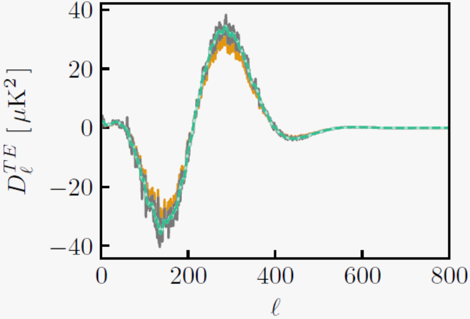

(beam transfer function not deconvolved)

- *TT* slightly affected
- *EE* lost power
- *BB* much larger (*EE* shape)
- *TE* slightly affected

ideal vs non-ideal output spectra

ideal and non-ideal TODs, both processed with **ideal** map-maker.

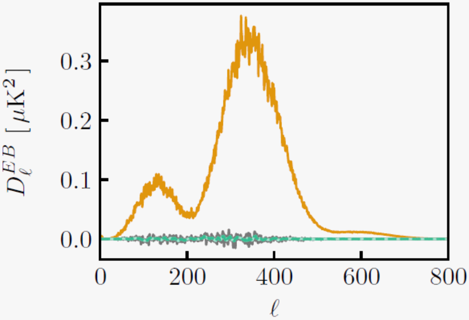

(beam transfer function not deconvolved)

- *TT* slightly affected
- *EE* lost power
- *BB* much larger (*EE* shape)
- *TE* slightly affected
- *EB* non-zero!

ideal vs non-ideal output spectra

ideal and non-ideal TODs, both processed with **ideal** map-maker.

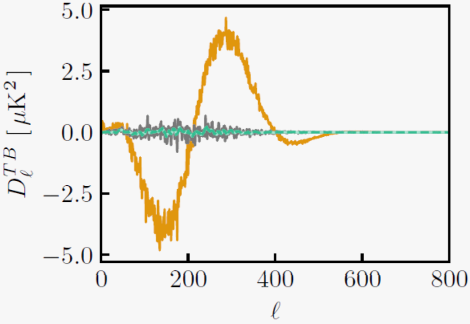

(beam transfer function not deconvolved)

- *TT* slightly affected
- *EE* lost power
- *BB* much larger (*EE* shape)
- *TE* slightly affected
- *EB* non-zero!
- *TB* non-zero!

how can we understand this?

modeling the observed maps

(minimal) TOD:	signal detected by 4 detectors.
map-maker:	bin-averaging assuming ideal HWP.
estimated output maps:	linear combination of $\{I, Q, U\}_{\text{in}}$.

for **good** coverage and **rapidly spinning** HWP:

$$\widehat{\mathsf{S}} \simeq \begin{pmatrix} m_{ii} I_{\text{in}} \\ [(m_{qq} - m_{uu}) Q_{\text{in}} + (m_{qu} + m_{uq}) U_{\text{in}}]/2 \\ [-(m_{qu} + m_{uq}) Q_{\text{in}} + (m_{qq} - m_{uu}) U_{\text{in}}]/2 \end{pmatrix} .$$

equations for the $\widehat{C}_\ell$s

Expanding $\widehat{S}$ in spherical harmonics:

$$
\begin{aligned}
\widehat{C}_\ell^{TT} &\simeq m_{ii}^2 C_{\ell,\mathrm{in}}^{TT},\\
\widehat{C}_\ell^{EE} &\simeq \frac{(m_{qq}-m_{uu})^2}{4} C_{\ell,\mathrm{in}}^{EE} + \frac{(m_{qu}+m_{uq})^2}{4} C_{\ell,\mathrm{in}}^{BB} + \frac{(m_{qq}-m_{uu})(m_{qu}+m_{uq})}{4} C_{\ell,\mathrm{in}}^{EB},\\
\widehat{C}_\ell^{BB} &\simeq \frac{(m_{qq}-m_{uu})^2}{4} C_{\ell,\mathrm{in}}^{BB} + \frac{(m_{qu}+m_{uq})^2}{4} C_{\ell,\mathrm{in}}^{EE} - \frac{(m_{qq}-m_{uu})(m_{qu}+m_{uq})}{4} C_{\ell,\mathrm{in}}^{EB},\\
\widehat{C}_\ell^{TE} &\simeq \frac{m_{ii}(m_{qq}-m_{uu})}{2} C_{\ell,\mathrm{in}}^{TE} + \frac{m_{ii}(m_{qu}+m_{uq})}{2} C_{\ell,\mathrm{in}}^{TB},\\
\widehat{C}_\ell^{EB} &\simeq \frac{(m_{qq}-m_{uu})^2-(m_{qu}+m_{uq})^2}{4} C_{\ell,\mathrm{in}}^{EB} - \frac{(m_{qq}-m_{uu})(m_{qu}+m_{uq})}{4} (C_{\ell,\mathrm{in}}^{EE} - C_{\ell,\mathrm{in}}^{BB}),\\
\widehat{C}_\ell^{TB} &\simeq \frac{m_{ii}(m_{qq}-m_{uu})}{2} C_{\ell,\mathrm{in}}^{TB} - \frac{m_{ii}(m_{qu}+m_{uq})}{2} C_{\ell,\mathrm{in}}^{TE}.
\end{aligned}
$$

analytical vs non-ideal output spectra

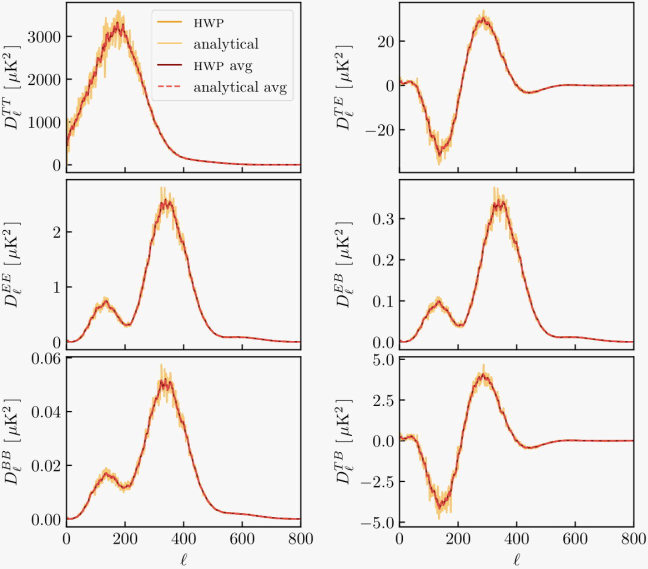

impact on cosmic birefringence

a side effect: measuring cosmic birefringence

CMB might also carry information about parity-violating new physics: **cosmic birefringence**.

(time-dependent parity-violating pseudoscalar field)

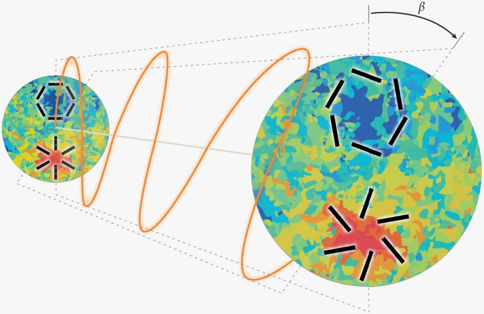

image credit: Yuto Minami;

a side effect: measuring cosmic birefringence

CMB might also carry information about parity-violating new physics: **cosmic birefringence**.

(time-dependent parity-violating pseudoscalar field)

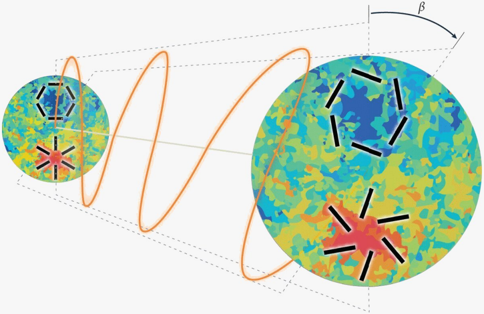

$$a^{E}_{\ell m,\mathrm{obs}} = a^{E}_{\ell m}\cos 2\beta - a^{B}_{\ell m}\sin 2\beta,$$
$$a^{B}_{\ell m,\mathrm{obs}} = a^{E}_{\ell m}\sin 2\beta + a^{B}_{\ell m}\cos 2\beta.$$

$$C^{EB}_{\ell,\mathrm{obs}} = \left(C^{EE}_{\ell} - C^{BB}_{\ell}\right)\sin 4\beta/2 + C^{EB}_{\ell}\cos 4\beta.$$

image credit: Yuto Minami;

a side effect: measuring cosmic birefringence

CMB might also carry information about parity-violating new physics: **cosmic birefringence**.

(time-dependent parity-violating pseudoscalar field)

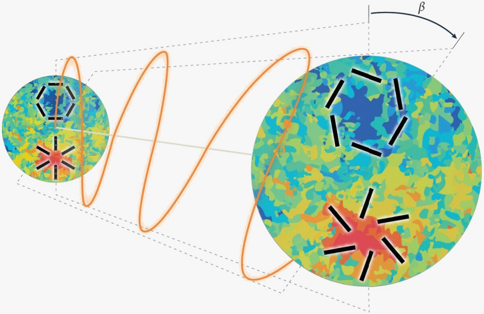

$$a^E_{\ell m,\mathrm{obs}} = a^E_{\ell m}\cos 2\beta - a^B_{\ell m}\sin 2\beta,$$
$$a^B_{\ell m,\mathrm{obs}} = a^E_{\ell m}\sin 2\beta + a^B_{\ell m}\cos 2\beta.$$

$$C^{EB}_{\ell,\mathrm{obs}} = (C^{EE}_\ell - C^{BB}_\ell)\sin 4\beta/2 + C^{EB}_\ell\cos 4\beta.$$

From *Planck* data:

$\beta = 0.35 \pm 0.14^\circ$ at 68% C.L.

↓

Constraint expected to **improve**.

image credit: Yuto Minami; Minami and Komatsu (2020) Phys. Rev. Lett. 125

HWP-induced miscalibration

Analytic $\widehat{C}_\ell$s satisfy the relations:

$$\begin{cases} \widehat{C}_\ell^{EB} \simeq \tan(4\widehat{\theta})/2 \left[\widehat{C}_\ell^{EE} - \widehat{C}_\ell^{BB}\right] \\ \widehat{C}_\ell^{TB} \simeq \tan(2\widehat{\theta})\,\widehat{C}_\ell^{TE} \end{cases}$$

our formulae suggest

$$\widehat{\theta} \equiv -\frac{1}{2}\arctan\frac{m_{qu}+m_{uq}}{m_{qq}-m_{uu}} \sim 3.8^\circ,$$

compatibly with simulations.

Degeneracy with cosmic birefringence
and polarization angle miscalibration!

In first approximation, HWP induces an additional miscalibration.

This doesn't mean that the HWP will keep us from measuring β,
but it shows how important it is to carefully calibrate $\mathcal{M}_{\mathrm{HWP}}$.

including frequency dependence

how does the map-model change

Without HWP: $$\begin{pmatrix} I_j \\ Q_j \\ U_j \end{pmatrix} = \sum_\lambda g_\lambda \begin{pmatrix} I_\lambda \\ Q_\lambda \\ U_\lambda \end{pmatrix} + n,$$

With HWP: $$\begin{pmatrix} I_j \\ Q_j \\ U_j \end{pmatrix} = \sum_\lambda \begin{pmatrix} g_\lambda^{ii} & 0 & 0 \\ 0 & g_\lambda^{qq-uu} & g_\lambda^{qu+uq} \\ 0 & g_\lambda^{qu+uq} & g_\lambda^{qq-uu} \end{pmatrix} \begin{pmatrix} I_\lambda \\ Q_\lambda \\ U_\lambda \end{pmatrix} + n,$$

where $$g_\lambda = \frac{\int \mathrm{d}\nu\, G(\nu) S_\lambda(\nu)}{\int \mathrm{d}\nu\, G(\nu)}, \quad g_\lambda^{ii} = \frac{\int \mathrm{d}\nu\, G(\nu) m_{ii}(\nu) S_\lambda(\nu)}{\int \mathrm{d}\nu\, G(\nu)},$$ and so on.

HWP non-idealities contribute to gain, polarization-efficiency and cross-polarization leakage.

effective SEDs

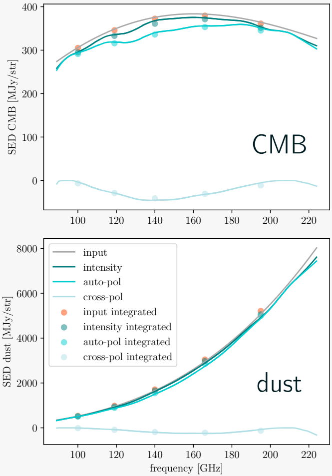

$$\sum_{\lambda} \begin{pmatrix} g_{\lambda}^{ii} & 0 & 0 \\ 0 & g_{\lambda}^{qq-uu} & g_{\lambda}^{qu+uq} \\ 0 & g_{\lambda}^{qu+uq} & g_{\lambda}^{qq-uu} \end{pmatrix} \begin{pmatrix} I_{\lambda} \\ Q_{\lambda} \\ U_{\lambda} \end{pmatrix} + n,$$

- Since all these effects are frequency dependent, they affect each component differently,
- An imprecise calibration of $\mathcal{M}_{\mathrm{HWP}}$ can lead to complications in the component separation step.

- we are now provided with a simulation pipeline that can be easily adapted to study more complex problems (adding noise, more realistic beams...);
- the analytical formulae represent an alternative tool to study the same problems more effectively (but approximately);
- obvious application: exploiting the analytical formulae to derive calibration requirements for the HWP Mueller matrix elements, so that they don't prevent us from measuring cosmic birefringence, nor spoil the foreground cleaning procedure.

backup

the idea

TOD: signal detected by 4 detectors looking at the same pixel;

Detected signal modeled as $d = (1\ 0\ 0) \cdot \mathcal{M}_{\text{det}} \mathcal{R}_{\xi-\phi} \mathcal{M}_{\text{HWP}} \mathcal{R}_{\phi+\psi} \cdot \mathsf{S}$;

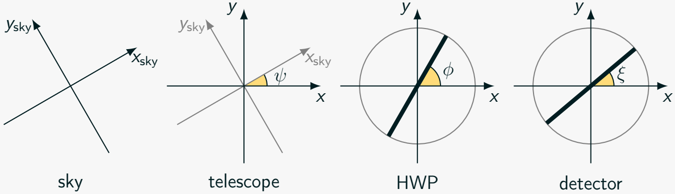

Apply a bin-averaging (ideal) map-maker to those 4 measurements.

$$\widehat{\mathsf{S}} \simeq \begin{pmatrix} m_{ii} I_{\text{in}} \\ [(m_{qq} - m_{uu}) Q_{\text{in}} + (m_{qu} + m_{uq}) U_{\text{in}}]/2 \\ [-(m_{qu} + m_{uq}) Q_{\text{in}} + (m_{qq} - m_{uu}) U_{\text{in}}]/2 \end{pmatrix}.$$

θ_{EB}, θ_{TB} and $\widehat{\theta}$

analytical expectation: $\widehat{\theta} \sim 3.8^\circ$.

compatible with best fit estimates!